Electrical Conduction and Dielectric Breakdown in Aluminum Oxide Insulators on Silicon

James Kolodzey, *Senior Member, IEEE*, Enam Ahmed Chowdhury, Thomas N. Adam, Guohua Qui, I. Rau, Johnson Olufemi Olowolafe, John S. Suehle, *Senior Member, IEEE*, and Yuan Chen

Abstract—Leakage currents and dielectric breakdown were studied in MIS capacitors of metal—aluminum oxide—silicon. The aluminum oxide was produced by thermally oxidizing AlN at 800–1100 °C under dry O_2 conditions. The AlN films were deposited by RF magnetron sputtering on p-type Si (100) substrates. Thermal oxidation produced Al_2O_3 with a thickness and structure that depended on the process time and temperature. The MIS capacitors exhibited the charge regimes of accumulation, depletion, and inversion on the Si semiconductor surface. The best electrical properties were obtained when all of the AlN was fully oxidized to Al_2O_3 with no residual AlN. The MIS flatband voltage was near 0 V, the net oxide trapped charge density, Q_{ox}, was less than 10^{11} cm^{-2}, and the interface trap density, D_{it}, was less than 10^{11} cm^{-2} eV^{-1}. At an oxide electric field of 0.3 MV/cm, the leakage current density was less than 10^{-7} A cm^{-2}, with a resistivity greater than 10^{12} Ω-cm. The critical field for dielectric breakdown ranged from 4 to 5 MV/cm. The temperature dependence of the current versus electric field indicated that the conduction mechanism was Frenkel–Poole emission, which has the interesting property that higher temperatures reduce the current. This may be important for the reliability of circuits operating under extreme conditions. The dielectric constant ranged from 3 to 9. The excellent electronic quality of aluminum oxide may be attractive for field effect transistor applications.

Index Terms—Dielectric breakdown, MIS capacitors, MOS capacitors, semiconductor-insulator interfaces.

I. INTRODUCTION

OVER the past decade, the gate oxides of field effect transistors in commercial integrated circuits have been scaled to below 4 nm thick to increase the gate capacitance and the transistor gain. In thin layers, the problems associated with gate electrode breakdown and leakage currents are crucial because of quantum mechanical tunneling. Under high electric field stressing, silicon dioxide degrades by the formation of traps, leading to lower breakdown fields [1]–[4]. After prolonged periods at relatively lower fields, SiO_2 may fail catastrophically by the mechanism of time dependent dielectric breakdown (TDDB), which is still not well understood [4]–[6]. Evidence indicates that the breakdown mechanism changes with the strength of the applied electric field, casting doubt on the suitability of high field stressing alone to predict the long-term reliability of circuits normally operating at lower fields [7]. High tunneling currents cause heating and waste power [8], and SiO_2 may have difficulty sustaining further scaling reductions in thickness. Oxide scaling to zero thickness produces essentially a metal-semiconductor transistor (MESFET) [9] that may not be desirable because of the well-known limitations in drive currents and transconductance compared to MOSFET's [10]. A larger dielectric constant increases the transistor gate capacitance with higher transconductance for the same dielectric thickness, or it can be thicker for the same capacitance with less tunneling leakage current, which decreases exponentially with thickness.

For device applications, various dielectrics have been investigated as alternatives to SiO_2. Oxidized AlAs is interesting for optical and electrical devices, but may contain residual arsenic [11], [12]. Tantalum pentoxide (Ta_2O_5) can be deposited at low process temperatures and has a dielectric constant above 25 depending on its structure, but may lack long-term stability against reactions with Si [13], [14]. Al_2O_3 deposited by sputtering is thermally stable and mechanically hard [15][16]. Simulations indicate that sputtered Al_2O_3 may be useful in the gates of flash memory circuits because its higher dielectric constant increases the capacitive coupling and increases circuit speed by three orders of magnitude, compared to using SiO_2 [17]. Unoxidized AlN has been used as a transistor gate dielectric on Si [18]. Previous studies of micron thick AlN films deposited by plasma enhanced chemical vapor deposition indicated resistance to oxidation up to 900 °C, with Al_2O_3 forming above 1100 °C [19]. In general, the defect density of deposited insulators is higher than that of thermally grown insulators.

This paper describes measurements of dielectric breakdown, leakage, and tunneling in Al_2O_3 produced by thermally oxidizing thin films of AlN on p-type Si substrates, as described previously [20]–[22]. We report on the defect density, dielectric constant, resistivity, and breakdown strength. In principle, aluminum oxide could be produced by other techniques including the reactive sputtering of Al metal in an oxygen atmosphere [23], and spray pyrolysis [24]. The optimum oxide process for applications is not clear, so it is valuable to compare methods. The best quality SiO_2 films are produced by thermal oxidation, which is the method explored here.

II. EXPERIMENTAL PREPARATION

The metal-insulator-silicon (MIS) capacitors were fabricated using the following procedure. First, p-type Si (100)

TABLE I
PROCESS DATA FOR OXIDIZED AlN SAMPLES INCLUDING SAMPLE NUMBER, AS-GROWN THICKNESS OF THE AlN, AND OXIDATION TEMPERATURES AND TIMES. THE SUBLAYER THICKNESS (d)WAS DETERMINED FROM ELLIPSOMETRY, STYLUS PROFILOMETRY, AND RBS DATA SIMULATED WITH RUMP SOFTWARE, ASSUMING A STRUCTURE HAVING THREE STOICHIOMETRIC LAYERS WITH THE COMPOSITIONS SHOWN HERE. THE SUBSTRATES WERE Si (100) WITH 1 Ω-cm RESISTIVITY

as-deposited		after oxidation			
Sample	AlN thickness (nm)	temp. / time (°C) / (hr)	d_{Al2O3} (nm)	d_{AlN} (nm)	d_{SiO2} (nm)
100601a	250	1100 / 2	435	0	144
100601b	250	1100 / 1	452	0	76
100601c	250	1000/ 1	378	6	42
100601d	250	900 / 1	90	203	0
100601e	250	800 / 1	25	236	0
012301a	55	900/ 1	101	0	0
012301b	55	900/2	101	0	0
012301c	55	900/ 3	101	0	0
SO-9001	-	900/ 1	-	-	27
SO-9002	-	900/ 2	-	-	43
SO-9003	-	900/ 3	-	-	56

substrates having a resistivity of 1 Ω-cm were degreased and acid cleaned using an RCA etch and an HF dip. The substrates were Si pieces roughly 1 cm wide. Layers of AlN were deposited by RF magnetron reactive sputtering using an Al metal target and a mixture of N_2/Ar gases with 0–25% Ar. The RF magnetron power was varied from 200 to 400 W, and the substrates were not intentionally heated during deposition. The thickness of the AlN films, given in Table I, was measured by mechanical stylus profilometry, with an accuracy of 5 nm. Atomic force microscopy (AFM) indicated that the surface roughness of the as-deposited layers was about 1 nm rms. X-ray diffraction (XRD) measurements indicated that the AlN structure varied from microcrystalline (weak, broad XRD peaks), to polycrystalline depending on the sputtering parameters. Higher RF powers and low pressures produced stronger AlN peaks. The AlN samples reported here had relatively weak XRD peaks, indicating microcrystalline structure with multiple orientations, but with the (110) plane preferentially oriented parallel to the (100) substrate. Additional details of the processing were given previously [20]–[22].

Oxidation was performed in a horizontal quartz furnace tube with dry O_2 at temperatures ranging from 800 to 1100 °C, for durations of 1–3 h. XRD measurements of the oxide showed relatively weak peaks corresponding to several phases including α-Al_2O_3 (sapphire), δ-Al_2O_3, and θ-Al_2O_3 [22], indicating that the oxide was microcrystalline and nearly amorphous. Table I shows the oxidation durations, temperatures, and the range of sublayer thickness. Shorter times and lower temperatures produced sublayers of incompletely oxidized AlN. Longer times and higher temperatures produced stronger Al_2O_3 peaks with fully oxidized AlN, and sometimes SiO_2 from the oxidation of the underlying Si substrate. The mechanism for the formation

of SiO_2 at the Si interface is not understood because the diffusivity of O in sapphire is negligible at 1100 °C ($D = 2 \times 10^{-16}$cm^2-s^{-1} at 1500 °C) [25]. It may be that the layers are porous.

The film composition was measured using Rutherford backscattering spectrometry (RBS), and secondary ion mass spectrometry (SIMS). The RBS data were analyzed using RUMP software simulations [26], which yielded thickness profiles with 10 nm accuracy for the layers reported here. RBS indicated that the as-deposited AlN was nearly stoichiometric with a few percent of oxygen, in agreement with the XRD data. The RUMP thickness values were calibrated by ellipsometry, profilometry and atomic force microscopy. To obtain the correct layer thickness using RUMP simulations, the density values for AlN and Al_2O_3 must be corrected manually by the user [27]. For samples in the 012 301 series and for samples 100 601d and e, there was no evidence for SiO_2.

The oxide was nearly stoichiometric Al_2O_3, with residual N less than 5% (the detection limit). As described previously [21], the thickness values given in Table I were simulated assuming three abrupt layers (Al_2O_3, AlN, and SiO_2) with no interface mixing. Therefore, the evidence for homogeneous layers thinner than 50 nm may not be physically valid because of interface roughness and composition mixing. AFM measurements indicated that the oxide surface roughness was about 1.2 nm rms.

Metal-insulator-silicon (MIS) capacitors were fabricated using standard optical lithography. Electrical contacts of 100-nm thick Al metal were evaporated onto the top of the oxide and onto the bottom of the Si substrate. Using photolithographic liftoff, the top contacts were patterned into circular dots with areas of 8×10^{-4}cm^2 for samples in the series 100 601, and 3.14×10^{-4} cm^2 for samples in the series 012 301.
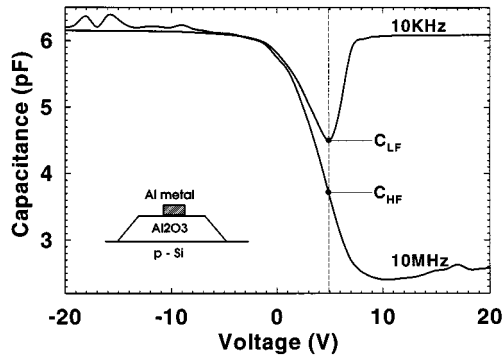
Fig. 1. The frequency dependence of the C–V characteristics at room temperature for an Al_2O_3 MIS capacitor with the AlN oxidized at 1000 °C for 1 h (sample 100 601c). The characteristics indicate the accumulation of holes at negative bias, the depletion of the Si surface at slightly positive bias, and the inversion of the Si surface at higher positive bias at low frequencies. The properties of the sample are given in Tables I and II. The relatively small flatband voltage corresponds to a low oxide defect density. The capacitances at low frequency C_{lf} and high frequency C_{hf} were used to calculate the interface trap density D_{it}. The inset shows the MIS structure with electrical contacts.

III. RESULTS

A. Capacitance–Voltage Measurements

The capacitance–voltage (C–V) characteristics yielded the bulk and interface defect densities of the oxide, and were measured versus applied bias and frequency using techniques described previously [28]. The applied ac voltage had a peak-to-peak altitude of 50 mV. Fig. 1 shows the C–V curves for a fully oxidized sample at high and low frequencies, exhibiting the Si surface charge regimes of electron accumulation, depletion, and inversion, similar to SiO_2 capacitors [29]. At negative dc bias, the net capacitance equaled the oxide capacitance C_{ox}, due to the accumulation of holes at the p-type Si surface. Slightly more positive voltages decreased the net capacitance due to the series connection of the oxide and the Si surface depletion capacitances. Higher positive voltages at frequencies less than the carrier generation rate increased the net capacitance to C_{ox} due to inversion of the Si surface with thermally generated electrons. Surface inversion indicates that transistor operation may be possible because the Fermi level is not pinned near midgap by defects. The frequency dependence of the inversion capacitance implied that the electron generation time was $t_{gen} = 1/100$ kHz $= 10^{-5}$ s. The frequency that produced quasi-static capacitance is relatively high at 10 KHz, indicating a short carrier lifetime, perhaps due to deep levels in the Si created during processing.

The flatband voltage is given by $V_{FB} = \Phi_{MS} - Q_{ox}/C_{ox}$, where Φ_{MS} is the Al-Si work function difference (−0.92 V for the metal and substrates used here), and Q_{ox} is the net oxide trapped charge density. In this analysis, Q_{ox} is the first moment of the oxide charge distribution divided by the oxide thickness, and encompasses all charged defects and impurities distributed throughout the oxide including surface states [29]. samples for which the AlN is fully oxidized have a small V_{FB} with the trapped charge density $(Q_{ox})/q$ below 10^{12} cm^{-2}, which is comparable to device-grade SiO_2 [29]. In Table II, the flatband voltage of smallest magnitude was obtained for the sample oxidized at 1000 °C, indicating that oxidized AlN can have a low

total defect density. We emphasize that Q_{ox} is not an interface parameter, but includes contributions from defects distributed throughout the oxide, and the defect density from the aluminum oxide would not be diminished even by the possibility of nearly ideal SiO_2 at the Si interface.

Comparisons between samples having the same thickness of AlN, but with different oxidation conditions, indicated that high temperatures and long times (sample 100 601) produced some SiO_2 at the Si interface and a low Q_{ox}. On the other hand, the under-oxidized sample (100 601) had a significantly higher defect density implying that the residual AlN at the Si interface is undesirable.

The density of interface traps, D_{it}, describes the quality of the Si surface. Due to their slower response time, interface traps produced a difference in the capacitances measured at low frequency C_{lf}, and at high frequency C_{hf}, as shown in Fig. 1. Using a standard approach, the frequency dependence of capacitance yields D_{it} at an energy in the gap determined by the total surface potential ϕ_s [30]

$$D_{it}(\phi_s) = (C_{ox}/q)(C_{lf}/(C_{ox} - C_{hf}) - C_{hf} \\ /(C_{ox} - C_{hf})) \quad (cm^{-2} - eV^{-1}) \quad (1)$$

where the applied gate voltage is $V_G - V_{FB} = V_{ox} + \phi_s$, and V_{ox} is the voltage drop across the oxide. The results in Table II are for ϕ_s near midgap where the defects have the most impact on device performance. D_{it} densities below 10^{11} cm^{-2} eV^{-1} indicated excellent interfaces, similar to device-grade SiO_2.

From the measured oxide capacitance and thickness, the dielectric constants in Table II ranged from 3 to 9, compared to 3.9 for SiO_2 [29]. The dielectric constant of sapphire (α-Al_2O_3) is 10.6 [31], but it is well know that the dielectric constants vary with microstructure for many materials. It may also be that the Al_2O_3 produced by thermally oxidizing AlN is less dense than sapphire.

B. Current–Voltage Measurements

Current–voltage (I–V) measurements were used to determine the dielectric breakdown strength and the electrical conduction mechanisms in the oxide. Using a voltage stress probe station described elsewhere [28], [32], the capacitors were biased into accumulation with the top metal contacts negative (−). The applied voltage was ramped at the relatively slow rate of 100 mV/s for better accuracy. In principle, a faster ramp rate would yield a higher breakdown field.

Fig. 2 shows the current density versus electric field (J–E) characteristics of several aluminum oxide samples, including the sample of Fig. 1 and an SiO_2 sample oxidized under similar conditions. The physical parameters of the samples are given in Table I. The electric field in the aluminum oxide was determined from the applied voltage using the thickness and the dielectric constants of the other layers ($\kappa = 9.1$ for AlN and 3.9 for SiO_2) [33]. The variation in J–E characteristics from sample to sample were attributed to differences in oxidation conditions, sublayer composition, and structure.

Table II summarizes the electrical results. The aluminum oxide had dielectric breakdown at fields ranging from 4 to 5 MV/cm. The leakage current densities were below 1.2×10^{-7}

TABLE II

THE DIELECTRIC PROPERTIES OF OXIDIZED AlN THIN FILMS OBTAINED FROM $C–V$ AND $I–V$ MEASUREMENTS OF MIS CAPACITORS. PRESENTED ARE THE SAMPLE NUMBER, OXIDE CAPACITANCE PER AREA, DIELECTRIC CONSTANT, FLATBAND VOLTAGE, NET OXIDE TRAPPED CHARGE, DENSITY OF INTERFACE TRAPS, RESISTIVITY AT 0.3 MV/cm, AND BREAKDOWN FIELD OF THE ALUMINUM OXIDE

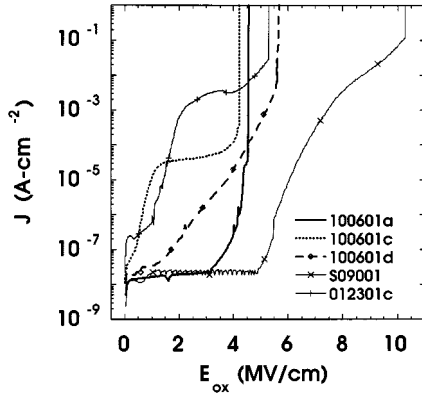| Sample	C_{ox} (nF-cm^{-2})	κ_{ox}	V_{FB} (V)	$(Q_{ox})/q$ (cm^{-2})	D_{it} (cm^{-2} eV^{-1})	ρ_{ox} (Ω-cm)	E_{BD} (MV/cm)
100601a	13.04	8.45	-1.67	1.46×10^{11}	2.26×10^{10}	2.2×10^{13}	4.6
100601b	13.2	7.9	-2.96	3.6×10^{11}	1.31×10^{10}	-	
100601c	20.5	9.77	+1.13	6.6×10^{11}	1.59×10^{11}	4.2×10^{12}	4.23
100601d	27.5	9.1	-18.1	2.84×10^{12}	1.04×10^{10}	1.6×10^{13}	5.67
100601e	30	8.8	-19.4	2.85×10^{12}	-	-	-
012301a						2.9×10^{12}	4.99
012301b	53	6.0	-3	7.0×10^{11}	7.25×10^{10}	3.5×10^{12}	4.94
012301c						1.3×10^{12}	5.32
SO9001						1.9×10^{13}	10.3
SO9002						2.8×10^{13}	
SO9003						3.5×10^{13}	8.27

Fig. 2. The dependence of leakage current density on oxide electric field for MIS capacitors with AlN oxidized at 1100 °C for 2 h, 1000 C for 1 h, and 900 °C for 1 h (samples 100 601a, c, and d, respectively), thinner AlN oxidized at 900 °C for 3 h (012 301c), and SiO$_2$ oxidized at 900 °C for 1 h (SO-9001). Properties are given in Tables I and II., and the shapes of the curves are discussed in the text. Dielectric breakdown occurred in the range from 4 to 5 MV/cm for the Al$_2$O$_3$, and near 10 MV/cm for the SiO$_2$.

A cm^{-2} at fields under 0.3 MV/cm, corresponding to resistivities ρ_{ox} greater than 10^{12} Ω-cm. The resistivities agreed reasonably with the published value for sapphire (10^{14} Ω-cm) but the breakdown strength of the samples was higher than the value accepted for bulk sapphire (0.5 MV/cm) [31].

Sample 100 601c has a current density that increased and then saturated at about 4×10^{-5} A cm^{-2} at fields near 1–3 MV/cm, and then increased again. This behavior is under study, but has been observed in ultrathin SiO$_2$ layers for which the constant current plateaus were attributed to phonon-assisted tunneling in neutral traps [2]. Another possibility for the current plateaus is series resistance in the test structure. For sample 100 601c, the increase in current at low fields may be due to breakdown at defects or weak spots in the dielectric, followed by a mechanism of self-healing [34], [35]. Small dark spots were observed by

visual microscopy on the metal surface, and it is possible that localized current surges evaporated small regions of the Al metal contact from the surface, preventing further conduction through that spot.

In comparison, the SiO$_2$ sample had relatively low current up to 5 MV/cm, followed by increasing current with dielectric breakdown near 10 MV/cm, in agreement with the accepted breakdown field of 10 MV/cm for thick SiO$_2$ [10]. Although the breakdown *field* of aluminum oxide was lower than for SiO$_2$, the breakdown *voltage* may be similar for optimized MIS devices having the same capacitance because of the higher dielectric constant of aluminum oxide.

C. Analysis of Leakage Current and Dielectric Breakdown

To determine the physical mechanisms responsible for leakage, the dependence of current on electric field was compared for two transport mechanisms known to be important for tunneling in insulators: Fowler–Nordheim (FN) tunneling and Frenkel–Poole emission.

The FN mechanism describes the tunneling of electrons from the metal into the conduction band of an insulator, with a dependence of current density on oxide electric field strength E_{ox} given by [10]

$$J_{FN} = a E_{ox}^2 \exp[-b/E_{ox}]. \tag{2}$$

The constants a and b are

$$a = q^2/(8\pi h \phi_b) = 1.538 \times 10^{-6}(\phi_b)^{-1} \text{A-V}^{-2} \tag{3}$$

and

$$b = 8\pi(2m^*)^{1/2}(q\phi_b)^{3/2}/(3hq)$$
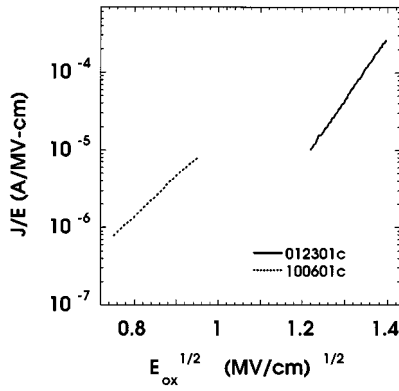$$= 68(m^*/m_o)^{1/2}(\phi_b)^{3/2} \text{ MV/cm} \tag{4}$$

where

Fig. 3. The current density versus electric field characteristics at room temperature for two aluminum oxide MIS capacitors (sample 100 601c oxidized at 1000 °C for 1 h and sample 012 301c oxidized at 900 °C for 3 h). Data are presented as a Frenkel–Poole plot showing the dependence of the leakage current density divided by the oxide electric field versus the square root of electric field. The linear slopes imply Frenkel–Poole emission in the Al_2O_3.
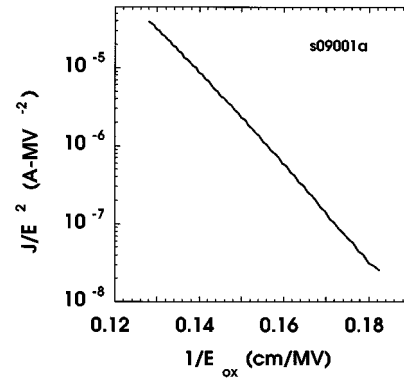

Fig. 4. The current density versus electric field characteristics of a SiO_2 MOS capacitor (sample SO-9001 oxidized at 900 °C for 1 h). Data are presented as a FN plot showing the dependence of leakage current density divided by the oxide electric field squared versus the reciprocal electric field. The linear slope implies FN tunneling in SiO_2.

h Planck's constant;

q magnitude of the electron charge;

$q\phi_b$ energy barrier height between the oxide and the metal contact (about 3.19 eV for Al on SiO_2 [36]);

m^* electron effective mass for tunneling;

m_o electron rest mass.

For SiO_2, the effective mass of a tunneling electron ranges from $m^* = 0.3m_o$ [37] to 0.5 m_0 [1].

Frenkel–Poole emission describes the field enhanced thermal excitation of trapped electrons into the oxide conduction band, with a dependence of current density on oxide electric field given by [10]

$$J_{\text{FP}} = cE_{\text{ox}} \exp[((dE_{\text{ox}})^{1/2} - \phi_t)q/k_bT] \qquad (5)$$

where

k_b Boltzmann's constant;

T measurement temperature;

c a constant that depeðds on the trap density N_t [38][39];

d $q/\pi\varepsilon_i$;

ε_i total electric permittivity of the insulator.

The energy $q\phi_t$ is the depth of the oxide trap potential well, which differs from the barrier height for FN tunneling in (2).

Unlike FN tunneling, Frenkel–Poole emission is explicitly temperature dependent; higher temperatures reduce the current and the effect of the field on the current. Both tunneling mechanisms, however, are affected by the temperature dependence of the bandgap, the barrier heights, and the carrier occupation statistics.

Fig. 3 shows a Frenkel–Poole plot [40] of current density versus oxide electric field for two aluminum oxide samples of different thicknesses at room temperature. Linear slopes imply Frenkel–Poole emission, which occurs at higher fields for the thinner aluminum oxide sample (012 301c). Frenkel–Poole emission is responsible for tunneling in Si_3N_4 [40]. Included purely for comparison, Fig. 4 shows a FN plot [28], [41] of current density versus oxide field for a conventional MOS
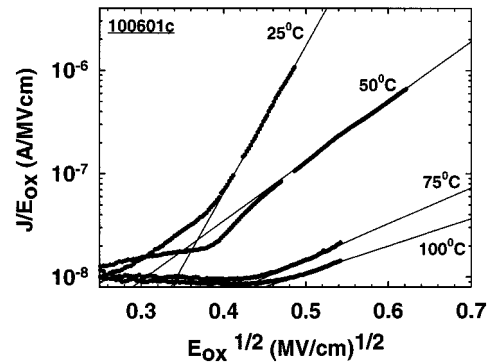

Fig. 5. Frenkel–Poole plot showing the current density versus oxide electric field characteristics at four measurement temperatures for an aluminum oxide MIS capacitor (sample 100 601c oxidized at 1000 °C for 1 h). Linear slopes and the strong dependence on temperature imply Frenkel–Poole emission.

capacitor of aluminum metal—SiO_2—Si. The linear slope covering several orders of magnitude corroborates FN tunneling in SiO_2. When presented as a FN plot, the aluminum oxide data was not linear, implying that FN tunneling did not occur in the aluminum oxide.

D. Temperature Dependence of Current–Voltage Characteristics

For further insight into the aluminum oxide conduction, the temperature variation of the J–E characteristics is presented as a Frenkel–Poole plot in Fig. 5. Linear regions imply Frenkel–Poole emission, with the current decreasing exponentially with temperature, as given by (5), with the effect of the electric field on the current being opposite to the effect of the trap depth. The terms in the numerator of the exponent in (5) can be considered as a field dependent effective activation energy, $E_{act} = q(dE_{\text{ox}})^{1/2} - q\phi_t$.

Fig. 6 presents an Arrhenius plot for the sample of Fig. 5, for currents at several electric fields below breakdown. The thermally activated behavior is consistent with Frenkel–Poole emission. The effective activation energy is related to the potential well depth $q\phi_t$ of the oxide traps and the square
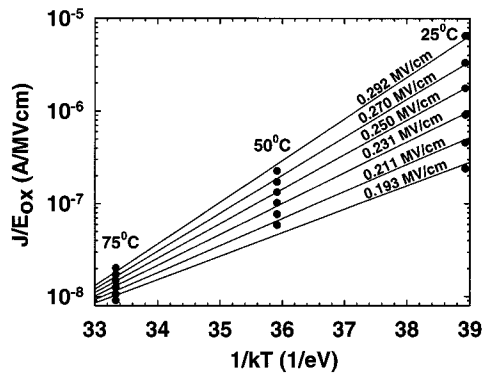
Fig. 6. Arrhenius plot of the aluminum oxide current at different values of electric field below breakdown for the sample of Fig. 5 (100 601c). Solid lines are the best fits to the experimental points. The slope implies thermally activated behavior, as discussed in the text.
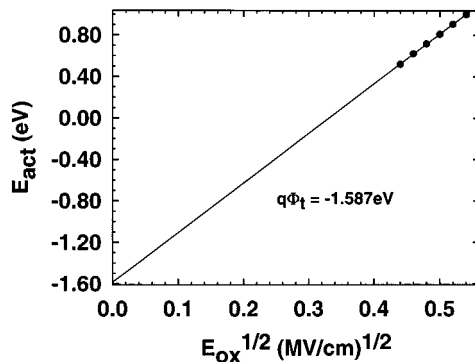

Fig. 7. Graphical determination of the Frenkel–Poole trap depth from the dependence of the effective activation energy on the square root of the electric field. By fitting the data to (5), the energy $q\phi_t = 1.6$ eV was obtained for the depth of the oxide trap potential well.

root of electric field. Fig. 7 show a graphical determination yielding $q\phi_t = 1.6$ eV. It is not yet clear if this energy is valid generally for aluminum oxide, or just for the particular samples measured here. For comparison, a 1.3 eV trap energy is reported for Si_3N_4 [40].

IV. DISCUSSION

At fields below breakdown, the Frenkel–Poole emission in Al_2O_3 is fundamentally different from conduction in SiO_2, which exhibits FN tunneling. The decrease in current with increasing temperature in Al_2O_3 may be important for circuit reliability under extreme conditions.

The dielectric constant of Al_2O_3 is generally higher than for SiO_2, so that gate dielectrics can be thicker for the same stored charge. For insulators less than 3 nm thick, tunneling occurs directly through the oxide with a probability that decreases exponentially with thickness. Thicker high dielectric gate insulators may be less susceptible to catastrophic failure and breakdown.

In principle, epitaxial techniques such as molecular beam epitaxy and chemical vapor deposition could be used to produce the starting layers of AlN for oxidation. The role of small amounts of N in oxidized AlN is unclear, but may be beneficial. It is well known that annealing SiO_2 in an N ambient reduces the defect density [29], and that the nitriding of SiO_2 using N_2O improves circuit reliability [42], [43]. The carrier confinement properties of Al_2O_3 are expected to be similar to those of SiO_2 because the bandgap of Al_2O_3 is 8.7 eV [44], close to the 8–9 eV bandgap of SiO_2.

V. CONCLUSIONS

Aluminum oxide (Al_2O_3) was produced by thermally oxidizing AlN on Si substrates using oxidation conditions similar to those for SiO_2. MIS devices were fabricated and had $C–V$ characteristics that exhibited the voltage-controlled charge regimes of accumulation, depletion and inversion on Si surfaces, with low defect densities. The best samples had net oxide trapped charge densities below 10^{11} cm^{-2}, similar to device-grade SiO_2. The dielectric constants ranged from 3 to 9, implying that properly prepared Al_2O_3 can be thicker than SiO_2 for the same gate capacitance. Prior to breakdown, the conduction mechanism in Al_2O_3 was Frenkel–Poole emission, which is qualitatively different from breakdown in SiO_2. The results showed that Al_2O_3 has device-grade characteristics and holds great promise for applications including gate dielectrics for field effect transistors.

REFERENCES

[1] D. J. DiMaria, E. Cartier, and D. Arnold, "Impact ionization, trap creation, degradation, and breakdown in silicon dioxide films on silicon," *J. Appl. Phys.*, vol. 73, pp. 3367–3384, 1993.

[2] K. Sakakibara, N. Ajika, K. Eikyu, K. Ishikawa, and H. Miyoshi, "Quantitative analysis of time-decay reproducible stress-induced leakage current in SiO_2 films," *IEEE Trans. Electron Devices*, vol. 44, pp. 1002–1008, 1997.

[3] I.-H. Chen, S. E. Holland, and C. Hu, "Electrical breakdown in thin gate tunneling oxides," *IEEE Trans. Electron Devices*, vol. ED-32, pp. 413–416, 1985.

[4] P. Solomon, "Breakdown in silicon oxide—A review," *J. Vac. Sci. Technol.*, vol. 14, pp. 1122–1130, 1977.

[5] J. S. Suehle and P. Chaparala, "Low electric field breakdown of thin SiO_2 and films under static and dynamic stress," *IEEE Trans. Electron Devices*, vol. 44, pp. 801–808, 1997.

[6] J. R. Brews, "The submicron MOSFET," in *High Speed Semiconductor Devices*, S. M. Sze, Ed, New York: Wiley, 1990.

[7] A. Martin, J. S. Suehle, P. Chaparala, P. O'Sullivan, and A. Mathewson, "A new oxide degradation mechanism for stresses in the Fowler–Nordheim tunneling regime," in *Proc. 1996 Int. Reliab. Phys. Symp.*, Dallas, TX, May 2, 1996, pp. 67–76.

[8] C. Hu, "Gate oxide scaling limits and projection," in *IEDM Tech. Dig.*, 1996, pp. 319–321.

[9] W. Frensley, private communication, 1998.

[10] S. M. Sze, *Physics of Semiconductor Devices*, New York: Wiley, 1981, p. 405.

[11] M. J. Ries, N. Holonyak Jr., E. I. Chen, and S. A. Maranowski, "Visible spectrum (650 nm) photopumped (pulsed, 300K) laser operation of a vertical cavity AlAs-AlGaAs/InAlP-InGaP quantum well heterostructure utilizing native oxide mirrors," *Appl. Phys. Lett.*, vol. 67, pp. 1107–1109, 1995.

[12] E. F. Schubert, M. Passlack, M. Hong, J. Mannerts, R. L. Opila, L. N. Pfeiffer, K. W. West, C. G. Bethea, and G. J. Zydzik, "Properties of Al2O3 optical coatings on GaAs produced by oxidation of epitaxial AlAs/GaAs films," *Appl. Phys. Lett.*, vol. 64, pp. 2976–2978, 1994.

[13] K.-W. Kwon, C.-S. Kang, S. O. Park, H.-K. Kang, and S. T. Ahn, "Thermally robust TaO capacitor for the 256-Mbit DRAM," *IEEE Trans. Electron Devices*, vol. 43, pp. 919–923, 1996.

[14] K.-M. Lin, C.-Y. Kwok, and R.-S. Huang, "Integrated thermo-capacitive type MOS flow sensor," *IEEE Electron Device Lett.*, vol. 17, pp. 247–249, 1996.

[15] J. W. Diggle and A. K. Vijh, Eds., *Oxides and Oxide Films*, New York: Marcel Dekker, 1976, vol. 4.

[16] G. T. Cheney, R. M. Jacobs, H. W. Korb, H. E. Nigh, and J. Stack, *IEDM Tech. Dig*, 1967.

[17] W.-H. Lee, J. T. Clemens, R. C. Keller, and L. Manchanda, "A novel high K inter-poly dielectric (IPD), Al2O3 for low voltage/high speed flash memories: erasing in msecs at 3.3 V," in *Tech. Dig. 1997 Symp. VLSI Technol.*, Feb. 1998, pp. 117–118.

[18] K. S. Stevens, M. Kinniburgh, A. F. Schwartzman, A. Ohtani, and R. Beresford, "Demonstration of a silicon field effect transistor using AlN as the gate dielectric," *Appl. Phys. Lett.*, vol. 66, pp. 3179–3181, 1995.

[19] F. Ansart, H. Ganda, R. Saporte, and J. P. Traverse, "Study of the oxidation of aluminum nitride coatings at high temperature," *Thin Solid Films*, vol. 260, pp. 38–46, 1995.

[20] E. A. Chowdhury, J. Kolodzey, J. Olowolafe, G. Qui, G. Katulka, D. Hits, M. Dashiell, D. van der Weide, C. P. Swann, and K. M. Unruh, "Thermally oxidized AlN thin films for device insulators," *Appl. Phys. Lett.*, vol. 70, pp. 2732–2734, 1997.

[21] J. Kolodzey, E. A. Chowdhury, G. Qui, J. Olowolafe, C. P. Swann, K. M. Unruh, J. Suehle, R. G. Wilson, and J. M. Zavada, "The effects of oxidation temperature on the capacitance-voltage characteristics of oxidized AlN films on Si," *Appl. Phys. Lett.*, vol. 71, pp. 3802–3804, 1997.

[22] E. A. Chowdhury, G. Qui, M. Dashiell, S. Woods, J. O. Olowolafe, D. van der Weide, C. P. Swann, K. M. Unruh, and J. Kolodzey, "Optical and electronic properties of oxidized AlN thin films grown at different temperatures," *J. Electron. Mater.*, vol. 27, pp. 918–922, 1998.

[23] J. Olowolafe, private communication, 1998.

[24] M. Aguilar-Frutis, M. Garcia, and C. Falcony, "Optical and electrical properties of aluminum oxide films deposited by spray pyrolysis," *Appl. Phys. Lett.*, vol. 72, pp. 1700–1702, 1998.

[25] K. P. R. Reddy and A. R. Cooper, "Oxygen diffusion in sapphire," *J. Amer. Ceram. Soc.*, vol. 65, pp. 634–638, 1982.

[26] L. R. Doolittle, "Rutherford universal manipulation program," *Nucl. Instrum. Meth. B*, vol. 9, pp. 344–351, 1985.

[27] V. Aubry-Fortuna, private communication, 1998.

[28] J. S. Suehle, P. Chaparala, C. Messick, W. M. Miller, and K. C. Boyko, "Field and temperature acceleration of time-dependent dielectric breakdown in intrinsic thin SiO2," in *Proc. 1994 Reliab. Phys. Symp.*, San Jose, CA, Apr. 12–14, 1994, pp. 120–125.

[29] E. H. Nicollian and J. R. Brews, *MOS Physics and Technology*, New York: Wiley, 1982.

[30] R. Castagne and A. Vapaille, "Description of the SiO2-Si interface properties by means of very low frequency MOS capacitance measurements," *Surf. Sci.*, vol. 28, pp. 157–193, 1971.

[31] *Handbook of Thin Film Technology*, L. I. Maissel and R. Glang, Eds., McGraw–Hill, New York, 1983, p. 6.12.

[32] P. Chaparala, J. S. Suehle, C. Messick, and M. Roush, "Electric field dependent dielectric breakdown of intrinsic SiO2 films under dynamic stress," *Proc. 1996 Int. Reliab. Phys. Symp.*, pp. 62–66, Apr. 30–May 2, 1996.

[33] O. Madelung, Ed., *Data in Science and Technology, Semiconductors, Group IV Elements and III-V Compounds*. Berlin, Germany: Springer–Verlag, 1991.

[34] D. J. Dumin, S. K. Mopuri, S. Vanchinathan, R. S. Scott, R. Subramoniam, and T. G. Lewis, "High field related thin oxide wearout and breakdown," *IEEE Trans. Electron Devices*, vol. 42, pp. 760–772, 1995.

[35] M. Nafria, J. Sune, D. Yelamos, and X. Aymerich, "Degradation and breakdown of thin silicon dioxide films under dynamic electrical stress," *IEEE Trans. Electron Devices*, vol. 43, pp. 2215–2226, 1996.

[36] T. Yoshida, D. Imafuku, J. L. Alay, S. Miyazaki, and M. Hirose, "Quantitative analysis of tunneling current through ultrathin gate oxides," *Jpn. J. Appl. Phys.*, vol. 34, pp. L903–L906, 1995.

[37] B. Brar, G. D. Wilk, and A. C. Seabaugh, "Direct extraction of the electron tunneling effective mass in ultrathin SiO2," *Appl. Phys. Lett.*, vol. 69, pp. 2728–2730, 1996.

[38] J. Frenkel, "On pre-breakdown phenomena in insulators and electronic semiconductors," *Phys. Rev.*, vol. 54, pp. 647–648, 1938.

[39] J. Frenkel, "On pre-breakdown phenomena in insulated and electronic semiconductors," in *Tech. Phys. USSR*, 1938, vol. 5, p. 2951.

[40] S. M. Sze, "Current transport and maximum dielectric ðtrength of silicon nitride films," *J. Appl. Phys.*, vol. 38, pp. 2951–2956, 1967.

[41] Y. Nissan-Cohen, J. Shappir, and D. FrℲan-Bentchkowsky, "Measurement of Fowler–Nordheim tunneling currents in MOS structure under charge trapping conditions," *Solid-State Electron.*, vol. 28, pp. 717–720, 1985.

[42] X. Zeng, P. T. Lai, and W. T. Ng, "AC hot-carrier- induced degradation in NMOSFET's with N2O-based gate dielectrics," *IEEE Electron Device Lett.*, vol. 18, pp. 39–41, 1997.

[43] X. Zeng, P. T. Lai, and W. T. Ng, "A novel technique of N2O treatment on NH3–nitrided oxide as gate dielectric for nMOS transistors," *IEEE Trans. Electron Devices*, vol. 43, pp. 1907–1913, 1996.

[44] P. Balk, *The Si/SiO2 System*. Amsterdam, The Netherlands: Elsevier, 1988.

James Kolodzey (M'74–SM'90) received the Ph.D. degree in electrical engineering from Princeton University, Princeton, NJ, in 1986 for research on SiGe alloys.

He was with IBM Corporation and Cray Research from 1975 to 1982. From 1986 to 1989, he was an Assistant Professor of Electrical Engineering at the University of Illinois at Urbana–Champaign, where he established a laboratory for high-frequency device measurements at cryogenic temperatures. In 1987, he worked on molecular beam epitaxy with Dr. A. Y. Cho at AT&T Bell Laboratories, Murray Hill, NJ. In 1990, he worked on SiC and SiGeC alloys with Dr. F. Koch and Dr. R. Schwarz at the Technical University of Münich, Münich, Germany. Since 1991, he has been at the University of Delaware, Newark. In 1997, he spent nine months at the University of Paris, Orsay, France, investigating optoelectronic devices. He is currently a Professor of Electrical and Computer Engineering at the University of Delaware. His research interests include the electrical and optical properties of alloys of group IV semiconductors, and their device and circuit applications. He is investigating aluminum oxide for transistor gate dielectrics and the properties of silicon carbide alloyed with germanium.

Enam Ahmed Chowdhury received the A.B. degree from Wabash College, Crawfordsville, IN, in 1995. Currently, he is pursuing the Ph.D. in physics at the University of Delaware, Newark.

Thomas N. Adam received the B.S. degree (Diplomingeneur) in electrical engineering from the Technical University of Chemnitz-Zwickau, Germany, in 1997. His research in the Department of Materials Science at the University of Delaware, Newark, focused on the electro-optical simulation of VCSEL diodes. His doctoral research with Prof. James Kolodzey in the Department of Electrical and Computer Engineering at the University of Delaware involves the growth of novel dielectric materials, such as Al2O3 for new MOS transistors.

Guohua Qiu received the B.S. and M.S. degrees in material science from Shanghai Jiao Tong University, Shanghai, China, in 1987 and 1990, respectively. He received the M.S. degree in electrical engineering from the University of Delaware, Newark, in 1997. His M.S. dissertation was on the investigation on $Al_xIn_{1-x}N$ and AlO_xN_y thin films.

From 1990 to 1995, he was a Lecture and Research Associate at Shanghai Jiao Tong University and engaged in research of intermetallic composite materials. He served as a Research Assistant at the University of Delaware from 1995 to 1997. He is currently a Product Engineer at Dallas Semiconductor, Dallas, TX.

I. Rau was born in Karl-Marx-Stadt, Germany, in 1975. He was admitted to the undergraduate program in physics at the Chemnitz University of Technology, Chemnitz, Germany, in 1993, where he is currently finishing his thesis to achieve the Dipl.-Phys. degree. His current research is focused on epitaxial silicide formation.

From 1997 to 1998, he was with the Department of Electrical and Computer Engineering, University of Delaware, Newark.

Johnson Olufemi Olowolafe received the Ph.D. degree in applied physics from the California Institute of Technology, Pasadena.

He was a World Trade Postdoctoral Fellow at the IBM T. J. Watson Research Center, Yorktown Heights immediately after graduation. After the postdoctoral training, he was a Senior Lecturer and Associate Professor at the University of Ife, Nigeria., from 1978 to 1989. During this period, he was a Visiting Research Associate Professor at Cornell University, Ithaca, NY, for a total of two years. From 1990 to 1995, he was with Motorola, Inc., Austin, TX, where he developed the copper interconnect metallization. Since 1995, he has been an Associate Professor of Electrical and Computer Engineering at the University of Delaware, Newark. His research interests include interaction of metals with elemental and compound semiconductors, Cu and Al interconnect metallization on microelectronic devices, development of novel gate electrode materials, and fabrication of semiconductor devices. He has coauthored over 100 journal articles and seven patents.

John S. Suehle (S'81–M'82–SM'95) received the B.S., M.S., and Ph.D. degrees in electrical engineering from the University of Maryland, College Park, in 1980, 1982, and 1988, respectively. In 1981, he received a Graduate Research Fellowship with the National Institute of Standards and Technology (NIST), Gaithersburg, MD.

Since 1982, he has been with the Semiconductor Electronics Division at NIST, where he is Leader of the Dielectric Reliability Metrology project. His research activities include failure and wear-out mechanisms of semiconductor devices and CMOS-compatible MEMS devices for *in situ* process monitoring. He serves as the chairman of the Oxide Integrity Working Group of the EIA/JEDEC 14.2 Standards Committee.

Dr. Suehle is a member of Eta Kappa Nu.

Yuan Chen received the B.S. and M.S. degrees in electrical engineering from Xi'an Jiaotong University, Xi'an, China, in 1989 and1992, respectively, and the Ph.D. degree in reliability engineering from the University of Maryland, College Park, in 1998. She conducted her postdoctoral research with NIST/UMCP and is currently with Bell Labs, Lucent Technologies, as a Member of Technical Staff. Her present research and projects cover wafer-level reliability testing and modeling, oxide reliability measurement, ultra-thin oxide characterization, hot-carrier aging, and failure analysis.